

# Fluctuation-regularized Front Propagation Dynamics

Elisheva Cohen and David A. Kessler

*Dept. of Physics, Bar-Ilan University, Ramat-Gan, IL52900 Israel*

Herbert Levine

*Center for Theoretical Biological Physics, University of California,  
San Diego, 9500 Gilman Drive, La Jolla, CA 92093-0319*

(Dated: November 4, 2018)

We introduce and study a new class of fronts in finite particle number reaction-diffusion systems, corresponding to propagating up a reaction rate gradient. We show that these systems have no traditional mean-field limit, as the nature of the long-time front solution in the stochastic process differs essentially from that obtained by solving the mean-field deterministic reaction-diffusion equations. Instead, one can incorporate some aspects of the fluctuations via introducing a density cutoff. Using this method, we derive analytic expressions for the front velocity dependence on bulk particle density and show self-consistently why this cutoff approach can get the correct leading-order physics.

Many physical, chemical, and biological systems exhibit fronts which propagate through space. Familiar examples range from chemical reaction dynamics such as flame fronts [1], phase transitions such as solidification [2], the spatial spread of infections [3], and even the fixation of a beneficial allele in a population [4]. In all these cases, the underlying dynamics of individual constituents (from molecules to organisms) gives rise multiple macroscopic states. It is thus of great interest to understand the universality classes of fronts which govern what will happen when systems such as these are prepared in a spatially heterogeneous manner. These classes determine the selection of propagation speed, the sensitivity to particle-number fluctuations, and the stability of the front with respect to deviations from planarity.

To date, several different classes of fronts have been described. Perhaps the simplest one, exemplified by the case of solidification, is that wherein a thermodynamically stable phase replaces a metastable one [2]. Here the mean-field front velocity is determined via the requirement that there exists a heteroclinic trajectory of the steady-state problem (obtained by assuming that all fields depend only on the traveling coordinate  $z \equiv x - vt$ ) connecting the metastable phase at  $+\infty$  with the stable one at  $-\infty$ . This type of front is robust with respect to fluctuations, with power-law corrections in  $1/N$  (where  $N$  is the number of particles per site in the final state) to the mean-field limit [5]. A second class is exemplified by the simple infection model  $A + B \rightarrow 2A$  on 1d lattice with equal  $A$  and  $B$  hopping rates [3]; this process leads in the mean-field limit to the well-known Fisher equation [4]  $\phi_t = r\phi(1 - \phi) + D\phi_{xx}$ . Here propagation is into the linearly unstable  $\phi = 0$  state and  $\phi$  is just the number of  $A$  particles at a site, normalized by  $N$ . Recent work [5, 6, 7, 8] has shown that the front behavior in the stochastic model does approach that of the Fisher equation, where the velocity is selected by the (linear) marginal stability criterion [9] to be  $2\sqrt{rD}$ , albeit with an anomalously long transient  $O(1/t)$  and anomalously

large fluctuation corrections  $O(1/\ln^2 N)$ . There are also some surprising findings in regard to both front stability in the case of unequal  $D$  [10], and also the scaling properties of front fluctuations [11]. Finally, there are also fronts which are determined by the nonlinear marginal stability criterion (for example, propagation into a nonlinearly unstable but linearly marginal state) which have properties intermediate to the previous two classes.

In this work, we introduce a new class of fronts corresponding to propagation up a reaction-rate gradient. We focus again on the  $A + B \rightarrow 2A$  reaction [3], with no  $A$  particles and an initial mean number  $N$  of  $B$  particles at all sites past some initial  $x_0$ , but now assume that the reaction probability depends on spatial position. The two situations we wish to consider are respectively the absolute gradient and the quasistatic gradient

$$\begin{aligned} r_a(x) &= \max(r_{\min}, r_0 + \alpha x) , \\ r_q(x) &= \max(r_{\min}, \tilde{r}_0 + \alpha(x - x_f)) \end{aligned} \quad (1)$$

where  $x_f(t)$  is the instantaneous position of the front, which we identify as  $x_f = \frac{1}{2} \sum_{i=0} N_A(x_i)x_i / \sum_{i=0} N_A(x_i)$ , where on the lattice  $x_i = ia$ . (The minimum value of  $r$  is just there to ensure that the bulk remains stable for all  $x$  and plays no important role.) The quasistatic problem should lead to a translation-invariant front with fixed speed  $v_q(\tilde{r}_0, \alpha)$ , whereas the absolute gradient will lead to an accelerating front. In the latter case, one can imagine ignoring the acceleration, obtaining thereby an adiabatic approximation to the velocity  $v(t; r_0, \alpha) \simeq v_q(\tilde{r}_0(t), \alpha)$  where  $\tilde{r}_0(t) = r_0 + \alpha x_f(t)$ . As we will see, fluctuation effects are absolutely crucial as the naive mean-field theory gives rise to “irregular” fronts in a way which we will define shortly. It should be noted that glimpses of this new class were obtained in studies of models of Darwinian evolution [12, 13, 14], but no general understanding was attained.

In Fig. 1, we show numerical solutions of the mean field equation (MFE, here just the Fisher equation with

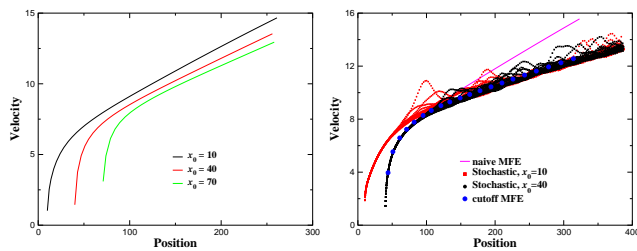


FIG. 1: Comparison of the MFE equation and the stochastic model, for  $D = 5$ ,  $r_0 = 1$  and  $\alpha = .02$ . (a) Numerical integration of the MFE, with initial conditions  $\phi = 1$  for  $x < x_0$ , 0 otherwise. (b) Twenty simulations of the stochastic system with  $N = 10^6$ , for each of two  $x_0$ 's,  $x_0 = 10, 40$ ; also plotted is the corresponding cutoff MFE graph with  $k = 0.3$ . We note in passing that the distribution of velocities seems highly skewed, with a large tail at velocities in excess of the mean.

spatially varying  $r$ ) versus a stochastic stimulation [5, 15] of the original continuous time Markov-process, both for the absolute gradient case. The MFE behaves *irregularly* in the sense that the front *never* recovers from its initial conditions, i.e. the system never falls into a dynamic attractor. Conversely, we define a *regular* front as one for which changes in initial data (as long as  $N_A$  remains zero past some starting point) can only effect a time-translation of an otherwise fixed front solution and hence would be invisible on a plot of velocity versus position. Clearly, the stochastic process gives rise to a regular front and thus cannot in any manner be approximated by the MFE.

To get some insight into the notion of regularity, we employ a heuristic approach in which we mimic the leading-order effect of finite population number fluctuations by introducing a cutoff in the MFE [12, 16, 17]. This cutoff replaces  $r(x)$  by zero if the density  $\phi$  falls below  $k/N$  for some  $O(1)$  constant  $k$ ; this change in the reaction term prevents the leading edge from spreading too far, too fast. This idea has proven its reliability in the Fisher system with *constant* reaction rate where it correctly predicts the aforementioned anomalous effects [6]. A numerical simulation of the cutoff equation reveals the recovery of regularity (see Fig. 2a) in its long-time behavior; of course, the time it takes to converge to the dynamic front attractor diverges as  $N \rightarrow \infty$  (data not shown). Returning to the simulation results in Fig 1b, we see that the cutoff MFE (using  $k$  as a fitting parameter) does a quantitatively accurate job of tracking the actual front dynamics. Fig. 2b presents a comparison of the front profile from the cutoff theory with that of the stochastic model; this was done for the quasistatic model as the translation invariance facilitates the necessary ensemble averaging. Overall, it is quite remarkable how well this simple approach works; later, we will use our analytic approach to the cutoff MFE to give at least some new indications of why this might be the case.

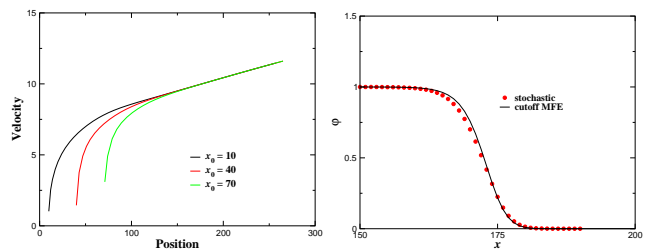


FIG. 2: (a) Regularity of the cutoff MFE; same parameters as Fig. 1a except for the cutoff of  $10^{-6}$ . (b) Average profile from twenty simulations of the (quasistatic) stochastic system with  $N = 10^6$ ; also plotted is the corresponding cutoff MFE graph with  $k = 0.3$

We next turn to using the cutoff MFE to study the front velocity. In Fig. 3, we present results for the front velocity at a fixed spatial position for the stochastic model and the cutoff mean field theory as a function of  $N$ . This is done both for the absolute gradient model and for the corresponding quasistatic model. From the data, we can draw the following conclusions. First, both models exhibit velocities which increase without bound as a function of  $N$ ; this is of course radically different than what has been encountered in the previous classes of propagating fronts. This behavior accounts for the fact that the long-time dynamics never approaches that predicted by the naive mean-field theory. Next, the two different models exhibit similar velocities at small  $\log N$  but become increasingly different as  $\log N$  goes to infinity. Finally, we note that at small enough  $\log N$ , the velocity can be approximated by just taking a cutoff version of the usual Fisher equation result for a *fixed* reaction rate  $r_F = r_0 + \alpha \bar{x}$ , i.e. completely neglecting the reaction-rate gradient across the front. This can be explained by noting that the effective interfacial width, the distance over which the particle density drops from its bulk value  $O(1)$  to its cutoff value  $O(1/N)$  scales as  $\log N$ ; hence one can neglect the gradient if  $\alpha \log N$  is small.

Given the highly unusual velocity results, an analytic treatment of the cutoff MFE at large  $N$  is clearly worthwhile. We restrict our attention to the quasistatic case where the problem is a “standard” one of finding a homoclinic trajectory in the traveling coordinate  $z$ . In what follows, it will become clear that spatial discretization effects cannot be neglected and hence we keep the explicitly discrete form of the hopping term, with lattice spacing  $a$ . The first key idea is that the nonlinearity is important only near the bulk state and in that region, diffusion is much less important than drift if the velocity is large. In this range of sites, then, the full equation

$$0 = D(\phi(z+a) + \phi(z-a) - 2\phi(z)) + v\phi' + r(z)(\phi - \phi^2)\theta(\phi - k/N). \quad (2)$$

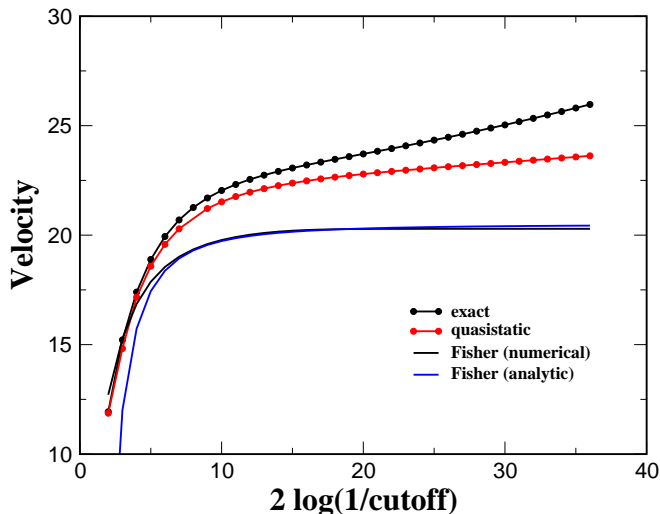


FIG. 3: Cutoff MFE equation for  $D = 5$ ,  $r_0 = 1$  and  $\alpha = 0.1$ , velocity at  $x = 200$  versus  $\log N$ . Shown for comparison is the absolute gradient model, the quasistatic model with  $\tilde{r}_0 = r_0 + 200\alpha$ , a numerical solution of a cutoff version of the usual Fisher equation with  $r_f = r_0 + 200\alpha$  and the Brunet-Derrida analytic approximation thereof.

can be solved by neglecting diffusion; this leads to

$$\ln\left(\frac{1-\phi}{\phi}\right) = \begin{cases} r_0(x + \alpha x^2/2)/v \\ r_{\min}(x - x_m)/v + r_0(x_m + \alpha x_m^2/2)/v \end{cases}$$

for  $x \geq x_m$  respectively, where  $x_m$  is the point where the minimum reaction rate is reached, i.e.  $r_0 + \alpha x_m = r_{\min}$ . We have chosen  $\phi(0) = 1/2$ , to fix the translation invariance, which is a slightly different definition of the front location, amounting to a small shift in  $r_0$ .

The above result needs to be matched to the solution near the cutoff point, where the nonlinearity can be dropped. As initially suggested by Rouzine, et al. [14], the resultant linear equation can be approached via the WKB ansatz  $\phi = e^{S(x)}$ , with the key observation that the cutoff point must occur close to the WKB turning point where  $\phi$  begins to oscillate. This is the only way that there is enough freedom to do the matching. The WKB equation takes the form

$$0 = \frac{4D}{a^2} \sinh^2(aS'/2) + vS' + r_0 + \alpha z. \quad (3)$$

Already at this point, we get a nontrivial result. We can de-dimensionalize this equation by introducing  $T = a/\ell S$ ,  $y = z/\ell$ ,  $\ell = v/(\alpha a)$  so that the equation reads

$$0 = \frac{4D}{va} \sinh^2(T'/2) + T' + y, \quad (4)$$

where the derivative is now w.r.t.  $y$  and we have dropped the small term  $r_0 a/v$ . [18] Thus,  $S$  (i.e.  $\ln N$ , once we do the matching) scales like  $D/(\alpha a^3)$  times a function of the dimensionless parameter  $va/D$ , so that the leading-order

results for all  $a$ , (for a given  $\alpha$  and  $D$ ) should lie on a universal curve. Furthermore, we recover the idea already discussed in Ref. ([14]) that  $a$  is a singular perturbation as far as the large velocity limit goes, since no matter how small  $a$  is, the parameter  $va/D$  eventually goes to infinity.

Returning to Eq. (3), the turning point is given by the discriminant equation  $\frac{dz}{dS'} = 0$ , yielding

$$0 = \frac{2D}{a} \sinh(aS'_*) + v, \quad (5)$$

which gives

$$S'_* = \ln\left(\sqrt{1 + \frac{v^2 a^2}{4D^2}} - \frac{va}{2D}\right). \quad (6)$$

If we match to the bulk solution near  $z = 0$ ,  $\phi$  declines by an amount related to the change in  $S$  from  $z = 0$  to the turning point  $z_*$ . This is given by

$$\begin{aligned} S_* &= \int_0^{S'_*} dS' S' \frac{dz}{dS'} \\ &= \int_0^{S'_*} \frac{dS'}{\alpha} S' \left[-\left(\frac{2D}{a} \sinh(aS') + v\right)\right] \\ &= -\frac{1}{\alpha} \left[ \frac{2D}{a^2} S'_* \cosh(aS'_*) - \frac{2D}{a^3} \sinh(aS'_*) + \frac{v}{2} (S'_*)^2 \right]. \end{aligned}$$

In the geometrical optics approximation,  $k/N \approx \phi(z_c) \approx \phi(z_*) = e^{S_*}$ , giving us an our lowest-order answer for the velocity. To improve upon this answer, one needs to both go beyond the geometrical optics approximation, and to develop a connection formula to go past the turning point. The latter involves writing  $\phi = e^{S'_* x} \psi$ , where  $\psi$  is smooth on the lattice scale [19], and showing that  $\psi$  satisfies an Airy equation. This procedure will be described in detail in a future publication[20], and here we just cite the results. The most significant correction, we find, comes from the further exponential decay, at rate  $S'_*$ , of  $\phi$  between the turning point and the cutoff point, which is near the zero of the Airy function solution to the  $\psi$  equation in the connection region. This gives an additional contribution of  $-S'_* \xi_0 (k/(D \cosh(aS'_*)))^{-1/3}$  to  $S$ , where  $\xi_0 = -2.3381$  is the location of the first zero of the Airy function. As already mentioned, the solution for the velocity is just  $\ln(N/k) = -S$ , so that the final expression becomes

$$\begin{aligned} \ln(N/k) &= \frac{1}{\alpha} \left[ \frac{2D}{a^2} S'_* \cosh(aS'_*) - \frac{2D}{a^3} \sinh(aS'_*) + \frac{v}{2} (S'_*)^2 \right] \\ &\quad - \xi_0 S'_* \left( \frac{\alpha}{D \cosh(aS'_*)} \right)^{-1/3} \end{aligned} \quad (7)$$

Let us examine the various limits of this expression. First, in the continuum limit,  $av/D \ll 1$ . Then  $S'_* = v/2D$ , so that  $aS'_* \ll 1$ . Then,  $S_* = (2D(S'_*)^3/3 +$

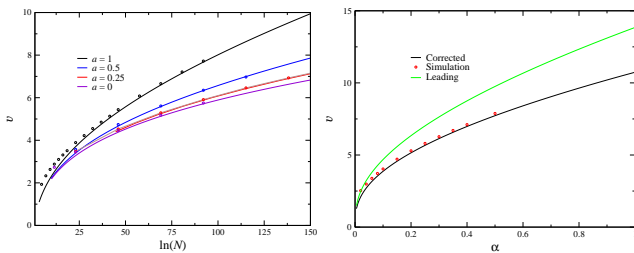


FIG. 4: (a) Velocity,  $v$ , vs.  $\ln(N)$  for lattice spacings  $a = 1, 0.5, 0.25$ , and  $0$ ,  $\alpha = 0.1$ ,  $D = r_0 = 1$ . from simulation, together with the analytic approximation Eq. (7) (b) Velocity,  $v$ , vs.  $\alpha$  at  $\ln N = 25$ , versus leading-order and full analytic expressions. In both figures,  $k = 1$ .

$v(S_*')^2/2)/\alpha$ ; the correction term is  $-S_*'\xi_0(k/D)^{-1/3}$ . Combining these gives the formula

$$v = 2(D^2 r_0 \alpha)^{1/3} \left[ (3 \ln(N/k))^{1/3} + \xi_0 (3 \ln(N/k))^{-1/3} \right]. \quad (8)$$

The scaling of  $v$  as  $\ln^{1/3} N$  is an agreement with the results of Tsimring, et al. for a continuum evolution model [12]. Now, as we mentioned above, for finite  $a$ ,  $av/D$  is eventually large for sufficiently large  $N$ . Then,  $S_*' = -\ln(va/D)/a$ . This gives  $S_* = v/(a^2 k)(-\ln(va/D) + 1 + \ln^2(va/D)/2)$ . Now, for very large  $va/D$ ,  $S_* \approx -v \ln(va/D)/(a^2 k)$ . However, this is only valid for  $\ln(va/D) \gg 2$ . In fact, it is a reasonable (20%) approximation only for  $\ln(va/D)$  bigger than 10, so that  $v$  would be unreasonably large. Thus, a strict asymptotic expansion is of no use. Our analytic results based on equation 7 are compared to numerical solutions in Fig.4; more details are given elsewhere [20]. Note that the full expression fits the data quite well, although the leading-order formula is not very accurate.

One of the most interesting aspects of the above calculation is that it does at all depend on form of the solution past the cutoff point; the mere existence of a cutoff is enough to force the system to the WKB turning point and hence fix the velocity. This is perhaps the reason why the cutoff MFE mimics the actual stochastic model; the fact that the region past the cutoff is in reality highly stochastic should not alter the velocity fixation which occurs in the part of space where fluctuation effects are indeed negligible. Turning this qualitative argument into a full theory remains a challenge for future work.

In summary, we have introduced a new class of fronts in reaction-diffusion systems and showed how fluctuations must be taken into account, even if only heuristically, if one wished understand their behavior. Using a cutoff

MFE approach, we can understand in detail the anomalous velocity behavior, at least for the quasistatic case. Further work should address the role of acceleration and front stability.

The work of HL has been supported in part by the NSF-sponsored Center for Theoretical Biological Physics (grant numbers PHY-0216576 and PHY-0225630).

- 
- [1] A. I. Kolmogorov, I. Petrovsky, and N. Piscounov, *Moscow Univ. Bull. Math. A* **1**, 1 (1937).
  - [2] D. A. Kessler, J. Koplik, and H. Levine, *Adv. Phys.* **37**, 255 (1988).
  - [3] J. Mai, I. M. Sokolov, and A. Blumen, *Phys. Rev. Lett.* **77**, 4462 (1996).
  - [4] R. A. Fisher, *Annual Eugenics* **7**, 355 (1937).
  - [5] D. A. Kessler, Z. Ner, and L. M. Sander, *Phys. Rev. E* **58**, 107 (1998).
  - [6] E. Brunet and B. Derrida, *Phys. Rev. E* **56**, 2597 (1997)
  - [7] U. Ebert and W. van Saarloos, *Phys. Rev. Lett.* **80**, 1650 (1998).
  - [8] L. Pechenik and H. Levine, *Phys. Rev. E* **59**, 3893 (1999).
  - [9] E. Ben-Jacob, H. Brand, G. Dee, L. Kramer, and J. S. Langer, *Physica D*, **14**, 348 (1985).
  - [10] D. A. Kessler and H. Levine, *Nature* **394**, 556 (1998).
  - [11] E. Moro, *Phys. Rev. Lett.* **87**, 238303 (2001).
  - [12] L. S. Tsimring, H. Levine and D. A. Kessler, *Phys. Rev. Lett.* **76**, 4440 (1996).
  - [13] D. A. Kessler, D. Ridgway, H. Levine, and L. Tsimring, *J. Stat. Phys.* **87**, 519 (1997).
  - [14] I. M. Rouzine, J. Wakeley, and J. M. Coffin, *Proc. Nat'l. Acad. Sci.* **100**, 587 (2003).
  - [15] The simulation is performed by alternating binomial processes for hopping (with probability per particle  $Ddt$  in each direction) with the reaction probability per B particle equal to  $1 - (1 - \frac{r dt}{N})^{N_A}$ . This form guarantees that the probability never exceeds unity and leads to the mean-field equation  $\rho_t \simeq \rho(1 - \rho/N) + D\rho''$ . Setting  $\phi = \rho/N$  leads to the Fisher equation.
  - [16] E. Brener, H. Levine, and Y. Tu, *Phys. Rev. Lett.* **66**, 1978 (1991).
  - [17] T. B. Kepler and A. S. Perelson, *Proc. Nat'l. Acad. Sci. USA*, **92**, 8219 (1995).
  - [18] The scaling derived here assumes  $\tilde{r}_0$  of  $O(1)$  and hence gives a velocity constant in time even when we choose  $\tilde{r}_0 = r_0 + \alpha t$  in the quasistatic approximation to the absolute gradient case. This will break down at large times. One can derive thereafter a new scaling assuming large  $\tilde{r}_0$  of  $O(v)$ ; this will be presented elsewhere [20].
  - [19] E. Cohen and D. A. Kessler, preprint (cond-mat/0301503).
  - [20] D. Kessler and H. Levine, in preparation.